

Fabrication and Characterization of Carbon Nanotubes-Zinc Oxide Structure by

Drop-drying and Ink Jet Printing

by

Pai Liu

A Thesis Presented in Partial Fulfillment
of the Requirements for the Degree
Master of Science

Approved May 2012 by the
Graduate Supervisory Committee:

Terry Alford, Chair
Amaneh Tasooji
Stephen Krause

ARIZONA STATE UNIVERSITY

August 2012

ABSTRACT

This thesis elaborates the application of carbon nanotubes (CNTs) and it is discussed in two parts. In the first part of the thesis, two types of CNTs inks for inkjet materials printer are prepared. They are both chemical stable and printable, effective and easily made. The sheet resistance of printed films decreases exponentially as the number of layers increases. In the second part of this study, CNTs/ZnO composite structures are fabricated to understand the electronic and optical properties. The materials were deposited by two different methods: drop-drying and RF magnetic sputtering system on flexible polymer substrates. To further increase the conductivity of the various layers of deposited CNTs films, electrical and optical characterizations are also done. This study establishes CNTs as a multi-functional semitransparent conductor, which can be deposited at room-temperature with other transparent conductive oxide (TCO) composites for application in flexible electronics and printed circuit and sensors.

DEDICATION

Dedicated to my family and friends for their support and love.

ACKNOWLEDGEMENTS

It is my honor to thank my research advisor Prof. Terry L. Alford for his constant guidance, continuous support, supervision, and encouragement. I learned a lot while working with him. It gives me pleasure to offer thanks to other committee members: Prof. Stephen Krause for his advice and teaching in MSE courses; Dr. Amaneh Tasooji for her interest in this project.

I thank Tim Karcher for the training and guidance with the sputtering system. I also acknowledge the help of Prof. David Wright, Prof. Nathan Newman, Karl Swiss for the training and usage of various instruments.

It is a privilege to express my deep gratitude towards all members and labmates in Prof. Alford's group: Rajitha Vemuri, Sayantan Das, Aritra Dhar, Chia-ling Fang, Shenke Zhang, and Winnie Mathews. They all helped me with various discussions and experiments and they are all terrific graduate students and researchers.

I thank all my friends in ASU, especially Tiantian Zhang, Xiaofeng Wang, Liuxian Zhang, and my roommate Yixue Zhang for being there to help me, share the joys in past two years. I enjoyed my life in ASU with your company. It is my honor to be your friend and neighbour. I thank you all, with all my heart.

Lastly, from the bottom of my heart, I am grateful to my family for always being there for me: My father Junxi Liu, mother Qiumei Xue, my fiancé Zhengxing Cui and many more family members. This is because of their love and support that I was able to make this achievement.

TABLE OF CONTENTS

	PAGE
LIST OF TABLES.....	viii
LIST OF FIGURES.....	ix
CHAPTER	
1 INTRODUCTION.....	1
I. Carbon Nanotubes Properties and Characterization.....	1
II. Multi-component Transparent Conducting Oxides.....	3
III. Inkjet Printing technology.....	7
2 COST-EFFECTIVE PRINTABLE CARBON NANOTUBE INKS FORMULATIONS WITHIN INKJET PRINTED CONDUCTIVE FILMS.....	11
I. Introduction.....	11
II. Experimental details.....	13
III. results and discussion.....	15
3 TRANSPARENT AND IMPROVED CONDUCTIVITY OF CNTS/ZNO IN FLEXIBLE ELECTRONICS.....	22
I. Introduction.....	22
II. Experimental details.....	23
III. Results and discussion.....	28

CHAPTER	PAGE
IV. Conclusion.....	38
4 SUMMARY OF RESEARCH WORK.....	39
REFERENCE.....	41

LIST OF TABLES

TABLE	PAGE
1.1 The comparison of various transparent electrodes.....	6

LIST OF FIGURES

FIGURE	PAGE
1.1. Dimatix Materials Printer DMP-2800.....	7
1.2 Reynolds and Weber numbers plotted in a coordinate system.....	9
2.1 CNTs pattern 5 mm×5 mm on photo paper by Inkjet printing, from left to right, printing 1 time, 3 replicates and 5 replicates.....	16
2.2 Image showing three drops ejected from a DOD printer at different stages of drop formation.....	16
2.3 Sheet resistance as a function of number of printing replicates.....	18
2.4 Optical micrography of printed CNTs layers. (a~b) Optical microscope micrographs of printed one layer, three layers on glass substrate. (c~d).....	19
2.5 Printed CNTs pattern on Si wafer and glass by Ink-B.....	20
3.1 Wetting and drop drying process and deposition CNTs.....	26
3.2 Normalized radius as a function of time.....	27
3.3 Resistivity as a function of number of CNTs layers.....	30
3.4 Hall mobility as a function of number of CNTs layers.....	30
3.5 Carrier concentration as a function of number of CNTs layers.....	31

FIGURE	PAGE
3.6 Transparent film with different thickness of CNTs.....	33
3.7 UV-Vis Transmittance spectra of ZnO, CNTs, CNTs/ZnO films with different CNTs thickness.....	34
3.8 Cross-section SEM image of CNTs/ ZnO thin films.....	36
3.9 SEM image of morphology of CNTs/ ZnO thin films.....	37

CHAPTER 1

INTRODUCTION

I. CARBON NANOTUBES PROPERTIES AND CHARACTERIZATION

Carbon nanotubes (CNTs) can be depicted as rolling concentric graphene layers which have a high aspect ratio¹. The diameter of hollow cylinder structures can be small to nanometers and the length is up to a centimeter. Due to the graphite-like electronic structure, many physical properties of CNTs related to the electronic band structure could be studied, such as field emission properties and optical properties. Especially depending on the electronic structure of CNTs, transistor effect and field emission are two significant phenomenas for the applications in electric engineering.

According to the number of the layers in one CNT, the CNTs can be distinguished as single wall (SWNTs), and multi-wall CNTs (MWNTs). The SWNTs are monolayer molecules which can be seen as rolling graphene. The MWNTs consist of several concentric layers of carbon seen as rolling graphite, and the separation distances between the layers are about 0.34 nm. Similar to graphite, the electronic properties of the MWNTs also present semi-metallic while the SWNTs can present both semi-metallic and metallic behavior. This property depends upon the

quality of structure, and high quality structures can behave as metallic SWNTs. For the metallic SWNTs, the electrons can flow through the axial distance with a collision, and it is conductive. For the semi-metallic SWNTs, the semi-conductive materials have a band gap about 0.6 eV based on the diameter of the tubes². Generally, the electrical properties of MWNTs is due to the combination of the conductive layers and the semi-conductive layers, and it is in the intermediate region between the metallic and semi-metallic. In the structure of SWNTs, interaction of layers exists and the diameters of the layers are up to a few nanometers reducing the band gap. Therefore, the difference of conductivity between the metal and the semiconductor for the MWNTs is lower than that of SWNTs.

To expand the range of CNTs application, several pre-treatment methods are designed and applied to get CNTs suspended in various solvent systems. Using long chain molecules as surfactants has also been reported³. The long chain molecules entwining onto nanotubes and connect solvent molecule with the function groups on the side chain, instead of the C-C structure. However, for application on electronic devices, the harsh treatment conditions would effect the resistivity of CNTs to some extent. The harsh conditions include oxidizing acid

(high concentrated nitric acid, sulfuric acid), and long time sonication. In the work of Ren⁴, the highest conductivity CNTs network is formed with least sonication times.

II. MULTI-COMPONENT TRANSPARENT CONDUCTING OXIDES

Transparent conducting oxides (TCO) comprise a class of materials that are unique in sense that two seemingly conjugated properties coexist. TCOs find applications in flat-panel displays, OLED, solar cells, electromagnetic shielding of cathode ray tubes used for video display terminals, electro-chromic windows, low-emissivity windows in building defrosting windows, oven windows, static dissipation, touch-panel controls and invisible security⁵. For the conductivity of the materials, which is the loss part of the refractive index or the extinction coefficient, has a major contribution. More precisely, highly conductive materials normally do not allow visible light transmission while the materials with high transparency, such as the oxide glass, are insulators. Thus, it is reasonable that studying materials which are either highly conductive or remarkable transparent is important and promising. To study the basic material structure is beneficial to retain the transparency with increasing conductivity. Many phenomenological approaches have been used to understand the relationship about the optical properties and the electrical properties. These approaches can be used to guide the

studies on the TCO materials. One of the approaches presenting conductivity is shown below:

$$\sigma = ne\mu \quad \text{Eq 1.1}$$

where the σ is the conductivity of the materials, n is the number of charge carriers, e is the quantity of the charge, μ is the mobility. All of the four parameters in the Eq 1.1 are used to characterize the charge transport in conductive materials. And in this equation the conductivity is related to the number of the charge carriers and the mobility of materials. The movement of the electrons in the conductive solid materials can be expressed by using the mobility. In the study of the film transparent electrodes, the TCO semiconductors, such as impurity-doped ZnO, In₂O₃, SnO₂ and multicomponent oxides composed of combinations of these binary compounds are the best candidates for practical use.

In the current manufacturing processes used in the industry, indium thin oxide (ITO) is the most widely used materials in the field of optoelectronic field⁶. With the highly increasing need of ITO, the replacement of the ITO is also compelling. When used in reducing atmospheres at high temperature, the stability of doped ZnO is better than that of ITO⁷. Besides, in the field of solar power, the doped ZnO films can be beneficial. The ZnO films can be produced for the thin film

solar cells at relatively low temperature that those required for traditional SiO₂ panels giving flexibility for usage of several substrates. The high radiation resistance and availability of large area substrate are also promising.

The comparison for various transparent electrodes has already been done by Hu,*et al.*⁸, represented in the Table 1.1:

Table 1.1 The comparison of various transparent electrodes

	Thickness (nm)	R_s (Ω /sq)	Transmittance at 550 nm (%)	Figure of Merit 550 nm, T^{10}/R_s	Conductivity (S/cm)	Carrier Density (cm^{-3})	Refs.
Carbon Nanotubes	25	200	80	0.54	2000	10^{17a}	9, 10
Graphene	10	1800	70	0.02	555	1.57	11, 12
Metal Nanowire or thin film (i.e., Ag or Cu)	10^b	22	88	12.66	45454	5.868×10^{22}	13
PEDOT	50	200	85	0.98	1000	-	14
ITO	50~120	10~300 ^c	88	0.93-27.85	$\sim 1000^d$	$\sim 10^{20}$	15, 16

^a The numbers are calculated using the formula $\text{Conductivity} = \mu en$ for carbon nanotubes

^b The average thickness is calculated from the geometric aperture of 90% and nanowire height of 100 nm.

^c The sheet resistance depends on substrate and process conditions.

^d on plastic

III. INKJET PRINTING TECHNOLOGY

Inkjet printing (IJP) is viewed as a versatile manufacturing tool for applications in materials fabrication in addition to its traditional role in graphics output and marking. In the last few years it has been used as a free-form fabrication method for building three-dimensional parts and is being explored as a way of printing electrical and optical devices, especially where they involve organic components⁹. The unifying feature in all these applications is the dispensing and precise positioning of very small volumes of fluid (1–100 pL) on a substrate, before transformation to a solid. The applications of inkjet printing to the fabrication of structures for structural or functional materials applications requires an understanding as to how the physical processes operate during inkjet printing interact with the properties of the fluid precursors used¹³.

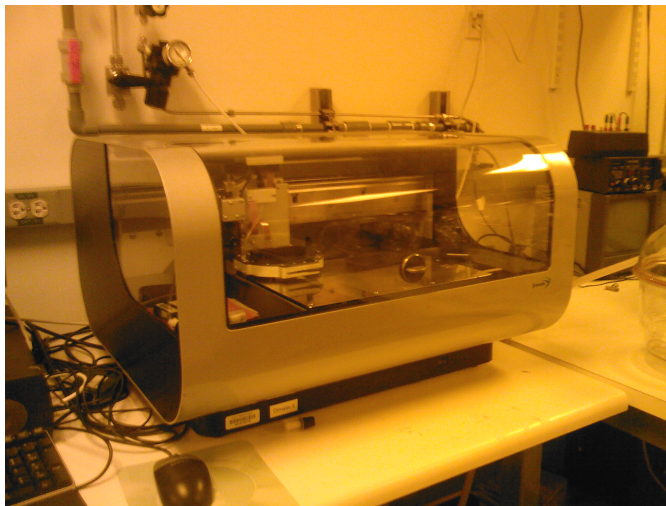


Figure 1.1. Dimatix Materials Printer DMP-2800

For printing free-forming materials and for multilayer devices, the need for a versatile inkjet technology generates a lots of problems that do not apply to conventional printing¹⁸. Higher resolutions will be needed, also, it must be possible to print pinhole-free layers. Multiple layers must be printed such that they mix and react to form a single material or such that they form discrete unmixed layers.

In general, ink properties will be matched to the performance of a specific printer. A typical ink has a viscosity up to 2 cP, but printers can be designed to handle liquids up to 100 cP¹⁸. The surface tension should not be lowered by surfactants because this leads to the ink wetting the faceplate around the nozzles and also prevents formation of a stable droplet stream. When the droplet hits the paper, it will be absorbed. Specially coated papers can limit the spread of the ink, and so improve resolution, by adsorbing the inks¹⁰.

The behavior of drops can be characterized by a number of dimensionless groupings of physical constants, introduced by Debye¹¹ in the Figure 1.2. The most useful of which are the Reynolds (Re), Weber (We), and Ohnesorge (Oh) numbers:

$$Re = \frac{v\rho a}{\eta} \quad \text{Eq 1.2}$$

$$We = \frac{v^2\rho a}{\gamma} \quad \text{Eq 1.3}$$

$$Oh = \frac{\sqrt{We}}{Re} = \frac{\eta}{(\gamma\rho a)^{1/2}} \quad \text{Eq 1.4}$$

where v is the velocity, and a is a characteristic length. ρ , η , and γ are the density, dynamic viscosity, and surface tension of the fluid, respectively. Together with the range of $Z = 1/Oh$ that allows stable printing, it can be plotted in a coordinate system defined by the Reynolds and Weber numbers to illustrate the regime of fluid properties where inkjet printing is possible in Figure 1.2²⁰.

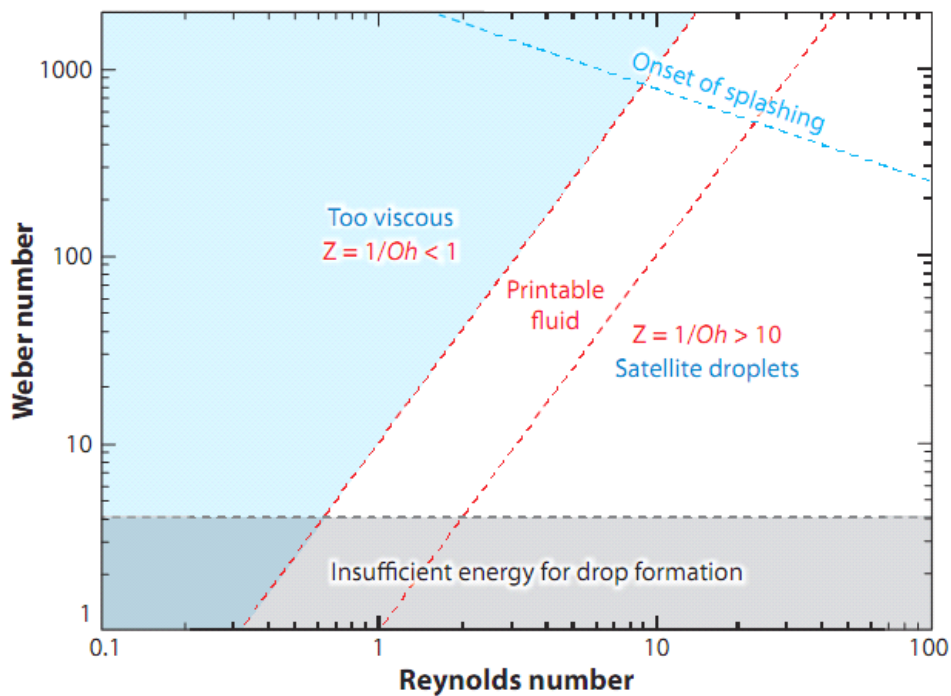


Figure 1.2 Reynolds and Weber numbers plotted in a coordinate system

However, the need to retain stability of the liquid droplets does make ink formulation much more difficult¹². Since sedimentation must be avoided in inks, particle sizes should be less than a micrometer. The dispersion must be very good to avoid any aggregation that would increase the viscosity and this starts to severely limit the maximum particle volume fraction for very small (100 nm) particles. The advantages of particulate suspensions include the greater chemical stability of crystal over solutions, the higher concentration of active species for most partially soluble compounds, and the greater ease of immobilizing species within a printed layer. There is much interest in conventional inkjet printing with nanoparticle inks¹³. There are two reports discussing this. The method has also been applied to printing electrodes for photovoltaic cells.

CHAPTER 2

COST-EFFECTIVE PRINTABLE CARBON NANOTUBE INKS

FORMULATIONS WITHIN INKJET PRINTED CONDUCTIVE FILMS

I. INTRODUCTION

Inkjet printing (IJP) has now become a very useful technology for depositing layers of conductive organic materials¹⁴. The method works by ejecting an ink through very fine nozzle, 22 μm in our case. The advantages of IJP over other thin film techniques lie in its patterning capability, the efficient use of materials. The low cost of the process, and in the fact that thin films can be printed on flexible substrates. Inks are selected based on several criteria. Three significant factors influence the quality of inkjet printing work: viscosity, surface tension of the ink, and together with the wettability of the droplets with substrate, which may affect the shapes and sizes of the printed dots.

Because of their exceptional electronic properties and mechanical strength¹, CNTs are attractive materials for nanotechnic applications. There are two categories of nanotubes: single-walled nanotubes (SWNTs), which consist of a single rolled-up sheet graphene; and multiple-walled nanotubes (MWNTs), which are depicted a

coaxial assembly of several graphene cylinders. As conductive wires, SWNTs offer attractive applications in micro- or nano-scale electronic devices. Many applications have now been suggested for nanotubes, because of the properties they present, including field-effect transistors, advanced composite materials and chemical sensors¹⁵.

For generating conductive multiple-walled carbon nanotubes pattern, here we study the usage of carbon nanotube as a cost-effective ink by inkjet printing on paper and other commonly used substrates. We use different substrates and different concentration inks to study the morphologies and electrical characteristics. However, the difficulties in processing these nanotubes are the key challenges for researchers working in this area. By overcoming their poor dispersibility in common solvents, the preparation of nanotubes dispersions is an essential requirement in the preparation. Vatjtai¹⁶ and Wei¹⁷ chemically modified multi-walled carbon nanotubes, to make them dispersible in water and usable as an ink. Some other research works published¹⁸, have led to the preparation of both SWNTs and MWNTs inks by using salmon sperm DNA and natural gums solutions¹⁹. While the fabrication involves the use of inexpensive printing cartridges and noncontact deposition onto substrates. Recent advances in nanotubes chemistry enable both the dissolution and dispersion of CNTs in

various solvent. These results suggest new alternative for fabricating CNT pattern by simply dispensing/printing the dissolved/dispersed particles on substrates.

In this step, thin films containing carbon nanotubes have been prepared using the inkjet printing technique. The inkjet printed films consist of small, randomly-oriented islands of nanotubes. The electrical characteristics of the films are measured at room temperature.

II. EXPERIMENTAL DETAILS

1. MWNTs ink preparation

The multiple -walled carbon nanotube was brought from 5 mg CNTs was dispersed in 5ml dimethylformamide (DMF). The mixture was sonicated for 30 min in room temperature followed by centrifuge for 5 min to remove some impurities or possible remaining CNT aggregates. The supernatant was collect. A small amount of the initial CNTs content was lost during this step. The final suspension obtained was opaque, black and stable. This ink is marked as *Ink-A*.

2. SWNTs ink

The 0.3 mg % CNTs were dispersed in a solution of 40 vol% ethanol and 40 vol% water and 20 vol% 1-cyclohexyl-2-pyrrolidone which the solvent, and the surfactant, respectively. The mixture was sonicated for 30 min at room temperature followed by a 5 min centrifuge to remove impurities or any remaining CNT aggregates. The supernatant was collected; however, a small amount of the initial CNTs content was lost during this step. The final suspension obtained was black, opaque and stable. This ink is marked as *Ink-B*.

A Dimatix Materials Printer DMP-2800 is used for the ink-jet printing. The accompanying 11610 Dimatix Materials Cartridge has a nozzle size of 22 μm and provided 10 pL per droplet.

Four-point-probe analysis, to determine the sheet resistance, was carrier out using a Keithley 2700 data acquisition system. Electrical resistivity, Hall mobility, and carrier concentration of the films were measured by Hall measurements in the van der Pauw geometry using an Ecopia HMS-3000 instrument.

III. RESULTS AND DISCUSSION

Figure 2.2 Droplet formation for the *ink-A* with pulse voltage of 30 V. Using the first CNTs/ DMF solution as an example. The liquid was ejected from the nozzle and a liquid column was formed. As time progressed the liquid column gradually formed a spherical head like at $t = 20\text{s}$. The maximum length of the ligament part is approximately $300\ \mu\text{m}$. Between 90 and 130 ms, the liquid column was completely separated from the nozzle. The drop watcher camera does not allow visualizing the contraction between the ligament part and the leading part to become a single droplet.

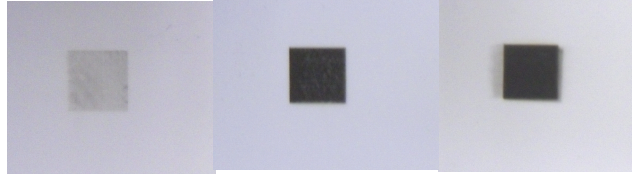


Figure 2.1 CNTs pattern 5 mm×5 mm on photo paper by Inkjet printing, from left to right, printing 1 time, 3 replicates and 5 replicates.

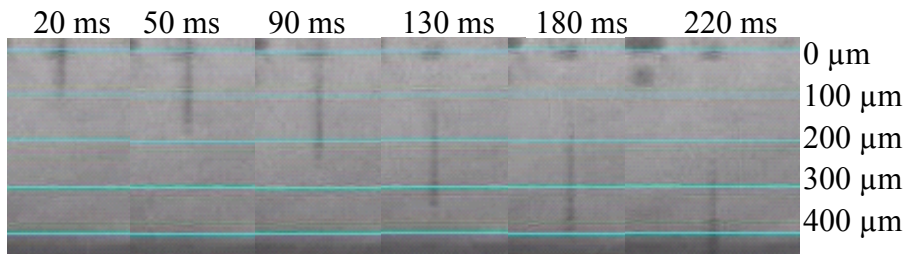


Figure 2.2 Image showing three drops ejected from a DOD printer at different stages of drop formation.

Figure 2.3 shows the relationship between printed layers and sheet resistance of printed CNTs. There are big improvements regarding to the ink reported in the literature⁸. the previous ink they used contained CNTs with acid treatment. As expected, the conductivity increases with the increasing number of print replicates. The decrease of resistance also accords with printed layers in an exponent by $\rho = 600 \cdot L^{-2.3}$ (L presents printed layer). Under the same condition, the sheet resistance of two different concentration of the *Ink-A* in this paper could be expressed as $\rho = 652.41 \cdot L^{-2.03}$. The sheet resistance decreases two and three order than the ones reported. For the one time printing CNTs layers, the sheet resistance in literature is 6×10^2 M Ω /sq, while in our case, the sheet resistance decreased to 0.72 M Ω /sq for Ink-A.

Figure 2.4 shows optical microscope top view of CNTs films with different printed layers on glass substrate. It can be observed that the film is continues and tidy edges compared with CNTs films on photo paper. Figures c~d show the optical microscope image of the same CNTs ink printed on photo paper. Because of the rough surface of photo paper, the edge of the printed pattern is not as smooth printed on glass. Bundles of CNTs are easily observed. The morphology of the paper substrate found to have the largest surface roughness (Figures 2.4 c and d). Both samples show 100% surface coverage by the CNTs ink.

Figure 2.5 shows the CNTs film we printed on Si wafer and glass by Ink-B. It proves that the ink we prepared could be printable and stable on several substrates.

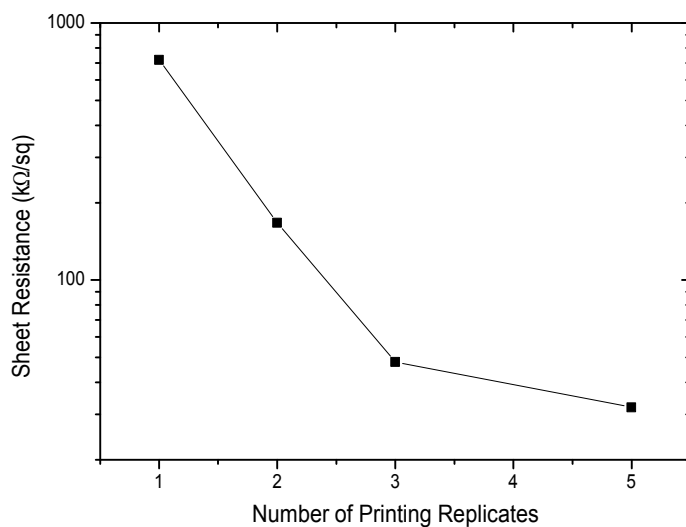


Figure 2.3 Sheet resistance as a function of number of printing replicates

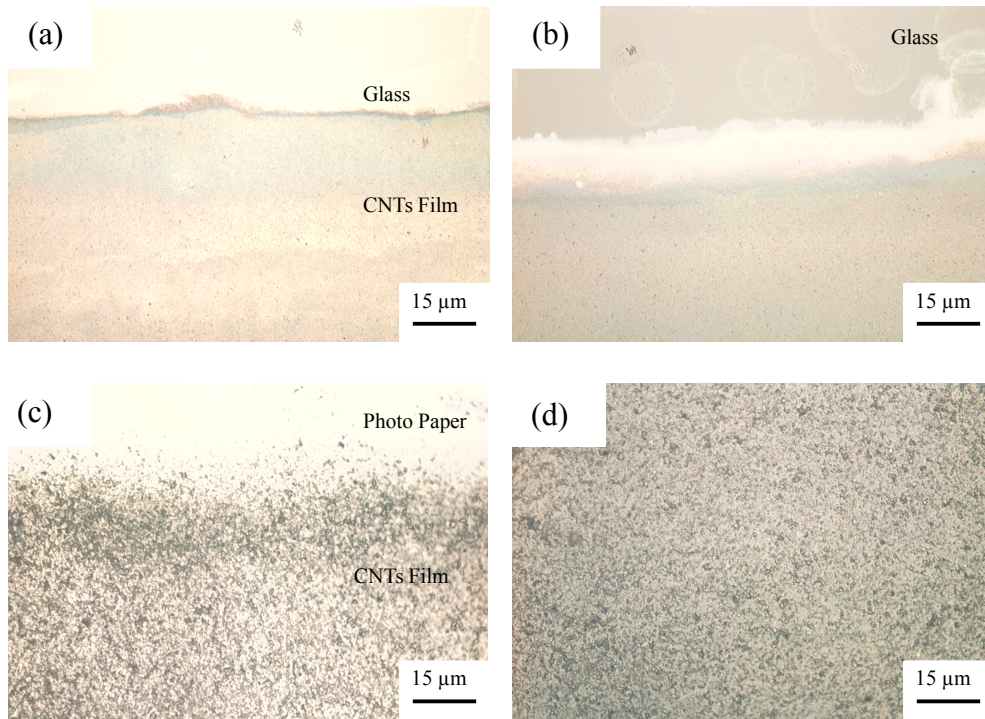


Figure 2.4 Optical microscope of printed CNTs layers. (a~b) Optical microscope micrography of printed one layer, three layers on glass substrate. (c~d) microscope images of the printed CNTs films on photo paper: the edge of pattern (c) and center (d)

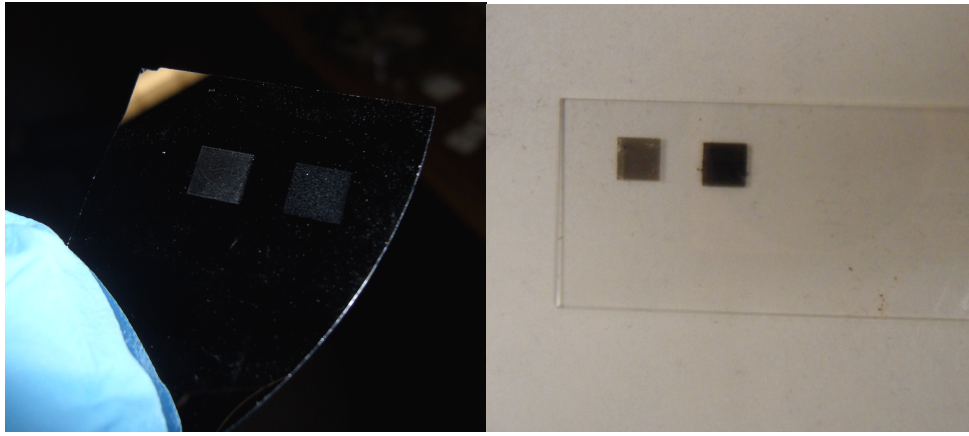


Figure 2.5 Printed CNTs pattern on Si wafer and glass by Ink-B

IV. CONCLUSION

Two kinds of relative stable CNTs based ink has been prepared and printed on various of substrates as conductive films. With increasing thickness of the printed layer, the electrical resistance of printed pads decreased exponentially. Because of the well formed CNTs layer without pre-treatment of CNTs nor long time sonication, we obtain lower sheet resistance value than reported in literature. The selection of inks is also based on several criteria, to form a uniform, continuous nanoparticle film. However in terms of aggregation property of CNTs itself, the CNTs inks we prepared and the inks introduced in other researches is facing the same problems is the stability of CNTs inks. Most of the inks until now are temporary stable and homogeneous and could only stand for about a few days. In our case, *Ink-A* could stand printable for 3 days, while *Ink-B* could stand for as long as 2 weeks, before injected into cartridges. For widely application of inkjet printing CNTs in industry, this issue is necessary to studied in further.

CHAPTER 3

TRANSPARENT AND IMPROVED CONDUCTIVITY OF CNTS/ZNO IN FLEXIBLE ELECTRONICS

I. INTRODUCTION

Transparent conducting oxides (TCOs) are characterized by high electrical conductivity approaching that of metals, and high transmittance ($> 80\%$) in the visible region of the electromagnetic spectrum. Many researchers are dedicated to improve the quality of TCOs for specify requirement of desired devices. The most common materials used as TCO is zinc oxide and its composites, due to its electronic and optics properties. Recent developments in the area of microelectronics on flexible substrates have been generated since flexible substrates can overcome the disadvantages of glass substrates²⁰. Polyethylene terephthalate (PET) and polycarbonate (PEN) have been widely researched as substrate materials for flexible electronics²⁹

Dielectric-metal-dielectric thin films have been studied in the hope of increased conductivity without significant losses in transmittance²⁹. TCO/Metal/TCO electronics as a substitution of TCO single layer with advantages of conductivity and transmittance. Various studies have been done using silver, copper and gold as

sandwiched metal layer, because of their excellent electrical properties²¹. Based on our group's research in these years, the transmittance and the sheet resistance change rapidly with layer thickness.

CNTs have attracted considerable attention because of their unique structure, high aspect ratio, and having extraordinary mechanical and electronic properties for many applications. In this work, single-walled carbon nanotubes (SWNTs) is deposited as the middle layer of TCO structure. compared with the similar structure of metals in electronic and optical properties. The structure will be deposited onto a flexible substrate.

II. EXPERIMENTAL DETAILS

Thin film layers of ZnO were deposited by rf magnetron sputtering onto PEN substrates at 10 mTorr pressure and 100 W power. 100 μm thick PEN (Dupont Teijin Films, Melinex Q65 with a adhesion promoting pretreatment on film side) substrates were used. Sputtering was preformed using ZnO as sputter targets.

Sputtering was done at a pressure of 10 mTorr in pure Ar. The thickness of ZnO outer layer was fixed at 35nm and thicknesses of CNTs layer were determined by cross-section SEM.

The CNTs were dispersed in 80 vol% ethanol as solvent and 20 vol% 1-cyclohexyl-2-pyrrolidone as the surfactant. The mixture was sonicated for 30 min in room temperature followed by centrifuge for 5 min to remove impurities or any possible remaining CNT aggregates. The supernatant was collect. And a small amount of the initial CNTs content was lost during this step. The final suspension obtained was opaque, black and stable.

The film of CNTs was deposited by drop-drying method²², with surface tension as internal force of CNTs solution. A certain volume of droplets of CNTs solution on the substrate were generated by pipettor. Because of the low contact angle of ethanol, the CNTs solution would spread on the substrate as film. To remove the solvent, drying by heat gun for 10 min. This procedure of dropping and drying was repeated for 1~3 times to obtain CNTs films with different thicknesses.

Figure 3.2 shows the drop radius (normalized by the initial radius) as a function of time. After about 360 s the drop attained a fixed base radius after 40 s. Drops of pure ethanol on the same substrate dried by maintaining a fixed base radius (25 mm in this case). Assuming quasistationary conditions, if diffusion of ethanol in air is rate controlling, then in a sessile drop receding with a constant contact angle the square of the base radius is linear with time²³. As the drying progressed further,

the drop attained a constant base radius at $t \sim 35$ s, and a surface undulation appeared at the top of the drop.

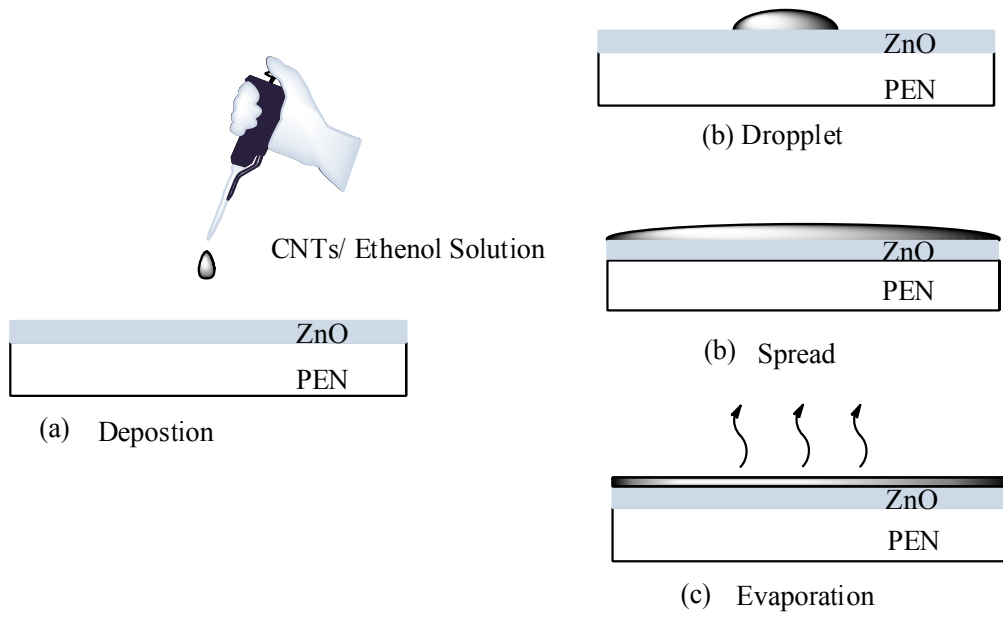


Figure 3.1 Wetting and drop drying process and deposition CNTs

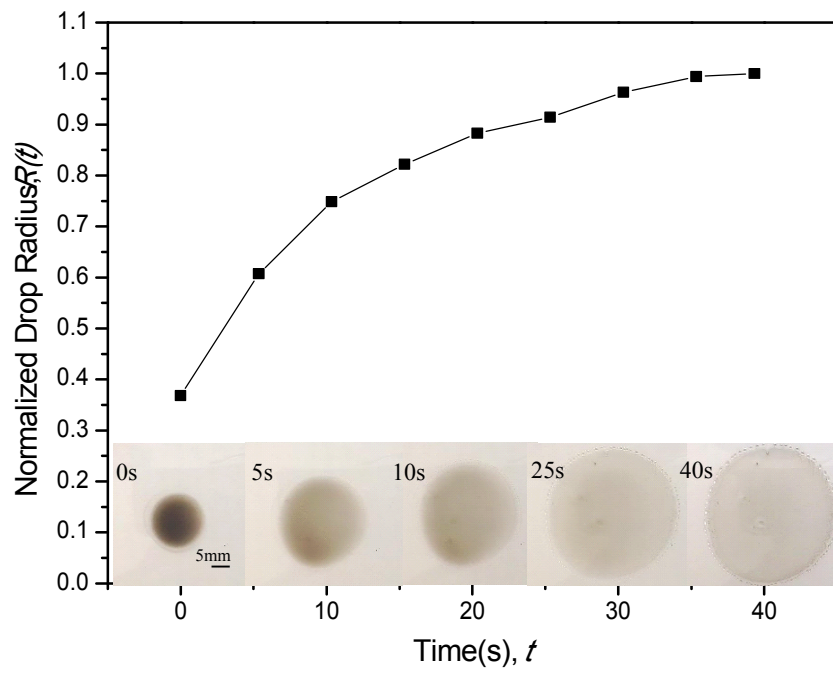


Figure 3.2 Normalized radius as a function of time

The optical transmittance, reflectivity, and absorbance of films were measured using an Ocean Optics double channel spectrometer (Model DS200) in the wavelength range of 300-900 nm with an aluminium mirror as the reference for reflectivity and air for transmittance. Tungsten-halogen and deuterium lamps were used for the visible and UV light sources, respectively.

Electrical resistivity measurements were obtained using a Hall effect measurement system. A Hall effect measurement system operating with a magnetic field of 0.51 T perpendicular to the sample surface was used to measure the carrier concentration by means of the van der Pauw method.

III. RESULTS AND DISCUSSION

Figure 3.3 shows the effect of number of CNTs layers as a function of resistivity. It is known that as-deposited ZnO films can vary greatly in their resistivity. For the as-deposited ZnO in previous study, the resistivity was 0.46 M Ω -cm for 60 nm of ZnO³⁰. As expected, the conductivity of the patterns increases with the number of CNTs layers. For the CNTs/ ZnO film on PEN, the resistivity decreases drastically from 0.46 M Ω -cm for no CNTs on top to 0.85 Ω -cm. The electrical resistivity decreases remarkably and then tends to be mildly to 0.18 Ω -cm with the increase of layers.

Figure 3.4 shows the variation of carrier concentration in the CNTs/ZnO films as a function of number of CNTs layer. The carrier concentration increases with increasing CNTs layers. The carrier concentration of the undoped ZnO layer on PEN is about $3 \times 10^{13} \text{ cm}^{-3}$. The carrier concentration of CNTs / ZnO structure with 3 layers of CNTs is $6.371 \times 10^{19} \text{ cm}^{-3}$, which is six orders of magnitude increase. However, it can be easily seen that the most significant increase happens when the CNTs layers just inserted. As the number of CNTs layers adding, there is a small rise in carrier concentration from one layer to three layers.

Figure 3.5 shows the variation of Hall mobility with number of CNTs layers. The Hall mobility of the as-deposited ZnO films is about $2.8 \text{ cm}^2/\text{V-s}$. The mobility slightly drops to $2.68 \text{ cm}^2/\text{V-s}$, when the first layer of CNTs was added. After that, the mobility increase with increasing layer of CNTs and reaches $7.32 \text{ cm}^2/\text{V-s}$ at three layer of CNTs/ ZnO.

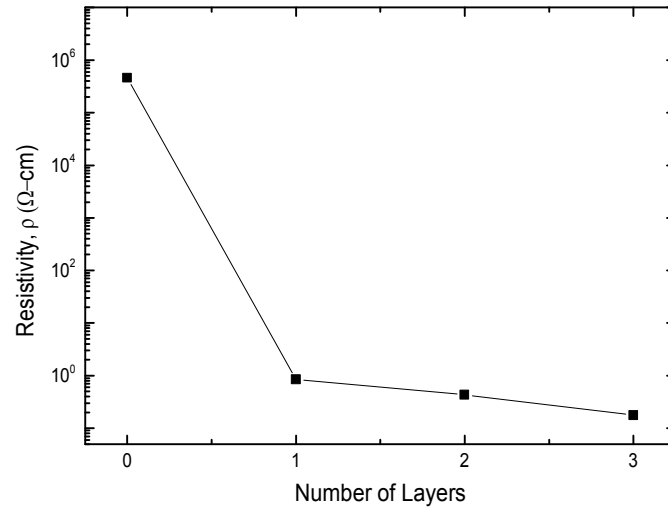


Figure 3.3 Resistivity as a function of number of CNTs layers

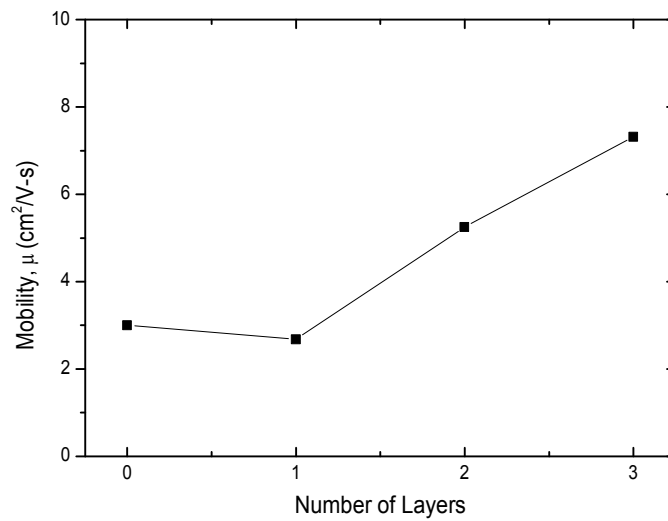


Figure 3.4 Hall mobility as a function of number of CNTs layers

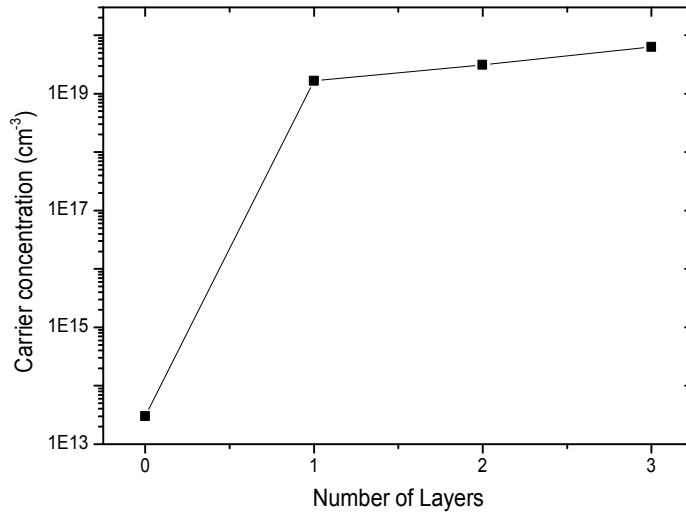


Figure 3.5 Carrier concentration as a function of number of CNTs layers

Figure 3.6 shows the transparent films we obtained with different number of CNTs layers. Figure 3.7 shows optical transmittance spectra from wavelength from 300 nm to 800 nm of CNTs/ZnO thin films on PEN for different thicknesses. The as deposited ZnO is about 80% transmittance over the visible range of wavelength (400~700 nm). The single undoped CNTs thin film also has a high transmittance of 90%, which is higher than as-deposited ZnO films. Upon insertion of a CNTs layer, the photopic average transmittance of the CNTs/ZnO multilayer drops to a value between 50% and 70%. In the UV and visible range, loss of transmittance is dominated by CNTs interband absorption⁶. It is also observed that there is an increase in transmission with increasing wavelength in the longer wavelength region.

Figure 3.8 is corresponding to the cross-section view of CNTs/ZnO films on glass. It can be clearly seen the bottom layer of ZnO with thickness of 35nm and SWNTs net-working. The exfoliated of SWNTs in Figure 3.8 are attributed to tension when cut the glass substrate, which also prove the existence of a firm and connected net working. The thickness of CNTs film could not be measured accurately because the top layer of ZnO formed a composite with the underlying ZnO film. The thickness of composite of ZnO and SWNTs is about 60 nm.

INTRODUCTION

ZnO/CNTs-1/ZnO ZnO/CNTs-2/ZnO ZnO/CNTs-3/ZnO

Transparent conductive oxides (TCOs) are materials that exhibit high transparency in the visible region along with high electrical conductivity. TCOs play an important role as transparent electrodes for flexible optoelectronic devices.

Figure 3.6 Transparent film with different thickness of CNTs.

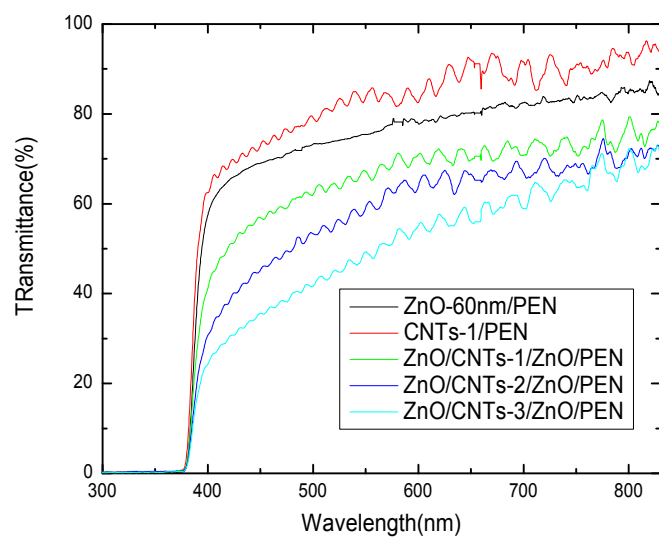


Figure 3.7 UV-Vis Transmittance spectra of ZnO, CNTs, CNTs/ZnO films with different CNTs thickness

Figure 3.9 shows SEM images of prepared films of different magnification. The CNTs are seen to be in the form of well connected net-working. The SWNTs appear as bundles (3~6 SWNTs in each bundle). But the bundles are thinner compared to those found in conventional dispersed films. The low degree of bundle is attributed to the surfactant SWNT dispersion that had most of the SWNTs present as individuals. The low degree of bundling of SWNTs can be potentially beneficial in preparing thin (~100 nm) optically transparent conductive films and coatings. ZnO was deposited on CNT net working by rf sputtering. The ZnO particles could easily filled into the space and gap between CNTs, and attached on SWNTs.

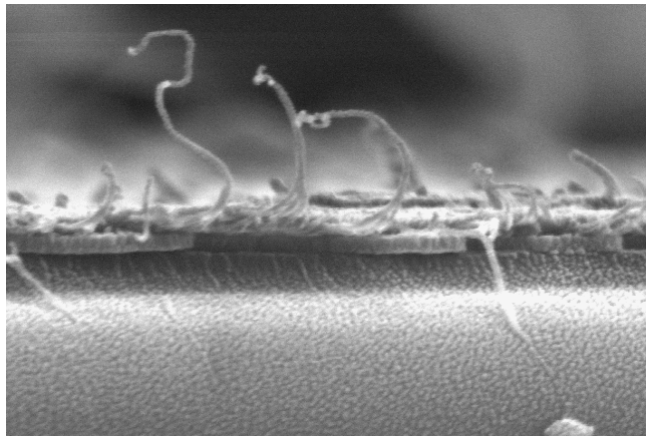


Figure 3.8 Cross-section SEM image of CNTs/ ZnO thin films

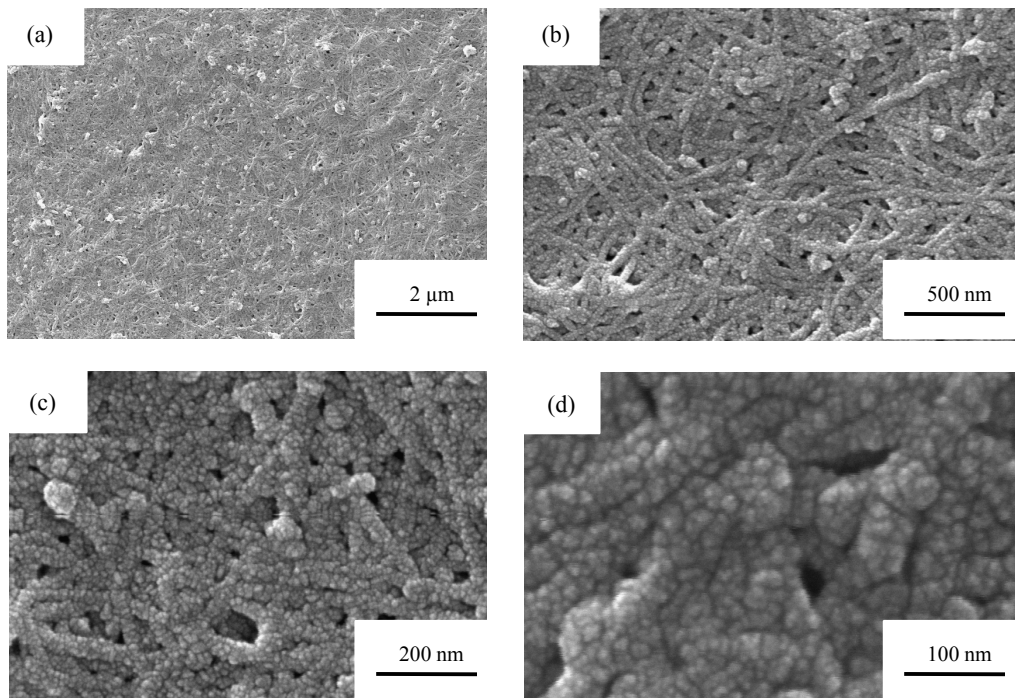


Figure 3.9 SEM image of morphology of CNTs/ ZnO thin films

IV. CONCLUSION

High conductivity CNTs/ZnO films with transparency property for optoelectronic device applications have been obtained by using the magnetron sputtering technique and drop-drying method. With high IR transmittance and low UV transmittance makes this device poor candidate for use as a UV transparent solar cell. However, the easy and effective deposition of CNTs thin films on different substrates (*i.e.*, glass, PEN, even ZnO, ITO) is still valuable and prospective. Because of the crossing in CNTs net-working, the structure loss transmittance in the UV region, which make CNTs thin films not comparable to metal thin film. Also we compare the electrical and optical properties of various transparent electrodes and compared their materials properties. This analysis provides positive information for people to choose transparent electrodes for various applications.

CHAPTER 4

SUMMARY OF RESEARCH WORK

In this study, application of CNTs in flexible electrode by various deposition methods is reported. First, CNTs/ZnO composite thin film to form a conductive and transparent electrode by drop drying and rf magnetic sputtering. The samples were characterized by hall measure and UV-Vis transmission to verify improved electrical and optical properties, respectively. Because of the net-working of CNTs film was formed as the increasing number of CNTs layers, the conductivity is increasing as expected. However, the decreasing of transmittance occurs in terms of CNTs' interband absorption.

Second two types of CNTs ink for Dimatix inkjet printer were prepared. CNTs could dispersed in a serial of organic solvent (*i.e.*, DMF, THF, absolute ethyl alcohol *et al.*) without any surfactant and keep the mixture stable for about 24 hour. The first CNTs ink is attempted based on this property, and it shows a improved conductivity for the printed pad by this ink.

The second ink is prepared based on an aqueous phase and 1-cyclohexyl-2-pyrrolidone as surfactant, followed by sonication and centrifuge. The morphology

image by optical microscope we got from these two inks prove the uniform conductive printed CNTs films. The inks also could be printed on various substrates and keep itself stable for 2 weeks. To further increase the conductivity of printed CNTs films, less pretreatment of CNTs and reducing the sonication time are necessary.

This study establishes CNTs as a multi-functional semitransparent conductor, which can be deposited at room-temperature with other TCO composites for applications in flexible electronic. So it can also be used as the printed circuit and sensor offering high conductivity.

REFERENCE

1. J. Khanderi, R. C. Hoffmann, A. Gurlob and J. J. Schneider, *J. Mater Chem.* **19**, 5039 (2009).
2. L. Hu, Y. Zhao, K. Ryu, C. Zhou, J. F. Stoddart and G. Grüner, *Adv. Mater.* **00**,1 (0000)
3. F. Xu, J. Xu, J. Ji, and J.C. Shen, *Colloids and Surfaces B: Biointerfaces* **67**, 1, 15, 67 (2008)
4. L. Ren, and S. Wang, *Carbon* **48**, 4397 (2010)
5. A. Catalano, C. Eberspacher, D. Ginley, T.M. Peterson and H.W. Schock, *MRS Proceedings* **426**: 419 (1996)
6. H. Han, D. Adams, J. W. Mayer and T. L. Alford, *Journal of Applied Physics* **98**, 8, 083705 (2005)
7. R. B. M. Cross, *Applied Physics Letters* **89**, 26, 263513 (2006)
8. L. Hu, D.S. Hecht, and G. Grüner, *Appl. Phys Lett.* **94**, 081103 (2009)
17. E. Tekin, Patrick J. Smith and Ulrich S. Schubert, *Soft Matter* **4**, 703 (2008)
10. (a) Y.-G. Tsai, M. Inoue, T. Colasurdo, *Tappi 99, Prep. Next Millennium*, Tappi Press: Atlanta, GA, 111 (1999)
(b) J. R. Boylan, *Tappi J.* **80**, 68 (1997)
11. B. Derby, *Annu. Rev. Mater. Res.* **40**, 395 (2010)
12. (a) M. D. Croucher, M. L. Hair, *Ind. Eng. Chem. Res.* **28**, 1712 (1989)
(b) R. Wong, M. L. Hair, M. D. Croucher, *J. Imaging Technol.* **14**, 129 (1988)
13. (a) A. D. Bermel, D. E. Bugner, *J. Imaging Sci. Technol.* **43**, 320 (1999)

-
- (b) J. Mendel, D. Bugner, A. D. Bermel, J. Nanopart. Res. **1**, 421 (1999)
14. N. H. Claudia, S. Pavel, A. C. Stelios and J. B. Christoph, Nano Lett. **8**, 9, 2806 (2008)
15. J. Li, Y. Lu, Q. Ye, M. Cinke, J. Han and M. Meyyappa, Nano Letters **3**, 7, 929 (2003)
16. K. Kordas, T. Mustonen, G. Toth, H. Jantunen, M. Lajunen, C. Soldano, S. Talapatra, S. Kar, R. Vajtai, P. M. Ajayan, Small **2**, 1021 (2006)
17. T. Wei, J. Ruan, Z. Fan, G. Luo, W. Fei, Carbon **45**, 2692 (2007)
18. W. R.; Panhuis, M. H. H. Small **3**, 9, 1500 (2007)
19. M. In Het Panhuis, A. Heurtematte, W. R. Small and V. N. Paunov, Soft Matter. **3**, 840 (2007)
20. H. Han N. D. Theodore T. L. Alford, J. of Applied Physics **103**, 013708 (2008)
21. K. Sivaramakrishnan and T. L. Alford, APPLIED PHYSICS LETTERS **94**, 052104 (2009)
22. R. Duggal, F. Hussain and M. Pasquali, Advanced Materials **18**, 1, 29 (2006)
23. F. Parisse and C. Allain, Langmuir **13**, 3598 (1997)